Engineering Solid Mechanics12 (2024) 207-220

Contents lists available at GrowingScience

Engineering Solid Mechanics

homepage: www.GrowingScience.com/esm

Numerical and analytical models of the mechanism of torque and axial load transmission in a shock absorber for drilling oil, gas and geothermal wells

Serhii Landar[a], Andrii Velychkovych[b*] and Vasyl Mykhailiuk[b]

[a]*National University "Yuri Kondratyuk Poltava Polytechnic", Ukrnaftagazservis Ltd, Ukraine*
[b]*Ivano-Frankivsk National Technical University of Oil and Gas, Ukraine*

ARTICLEINFO

Article history:
Received 14 October 2023
Accepted 9 March 2024
Available online
9 March 2024

Keywords:
Vibration protection
Drill shock absorber
Elastic element
Stick-slip
Screw pair
Contact pressure
Equivalent stresses

ABSTRACT

The paper proposes an improved design of a shock absorber used in drilling deep oil and gas and geothermal wells with polycrystalline diamond compact (PDC) bits. The proposed innovations successfully combat the dangerous phenomenon of self-excited vibrations, which can lead to malfunctions such as stick-slip and whirling of the drilling tool. Most conventional drill shock absorbers are designed to only absorb longitudinal vibrations, which was sufficient when using roller cutter bits for the drilling process. However, the design features of PDC bits and the phenomenon of interaction of their cutters with interlayered rocks during deep drilling impose new requirements on the properties of the drill shock absorber. To protect the downhole tool from abnormal torque values and torque oscillations, it is proposed to equip the shock absorber with a special torque transmission unit in the form of a fourteen-thread self-releasing screw pair. This unit is capable of transforming increases in external torque into increases in the force that loads the elastic element of the shock absorber. The numerical and analytical models of the mechanism of transferring external axial load and torque to the elastic element of the drill shock absorber are constructed. The distribution of contact pressures on the interacting surfaces of the screw pair and the distribution of equivalent stresses in the screw pair parts are analysed. The strength of the proposed drill shock absorber assembly was evaluated using the Huber-von Mises energy criterion. The dependence of the load transmitted to the elastic element of the shock absorber on changes in the external torque and external axial force is investigated. In general, it is determined that the external load is distributed evenly between all turns of the screw pair, and the limit state of the parts of the proposed assembly is not reached even under high-torque operating load. The obtained analytical dependencies will allow to effectively determine the required strength and stiffness of the elastic element of the drill shock absorber at the design stage. The obtained analytical results were verified using a finite element model.

1. Introduction

Today, for the efficient extraction of oil and gas and geothermal resources, deep vertical, directional and horizontal wells have to be constructed. Therefore, in practice, intelligent drilling is increasingly preferred (Li et al., 2022; Yavari et al., 2023), and to avoid problems with increasing drilling depths and constructing wells of complex configuration, advanced design tools and auxiliary highly specialised equipment are used (Haige et al., 2022; Maury et al., 2022; Velichkovic et al., 2018).

The peculiarities of the behaviour of long pipe strings under complex loads (Mao et al., 2024; Vytvytskyi et al., 2017; Shats'kyi & Struk, 2009) and the phenomenon of contact interaction of drilling tool elements with the wall and bottom hole (Bembenek et al., 2024; Grydzhuk et al., 2019) cause significant vibration loads. Vibrations have a harmful effect on drilling equipment, lead to significant energy losses and, in general, to a deterioration in the technical and economic performance of drilling (Saadat et al., 2023; Wang et al., 2023). The drilling industry has made significant progress in producing high-quality

* Corresponding author.
E-mail addresses: a_velychkovych@ukr.net (A. Velychkovych)

ISSN 2291-8752 (Online) - ISSN 2291-8744 (Print)

doi: 10.5267/j.esm.2024.3.002

bits, optimising the bottom of the drill string, and using ground controls to minimise vibrations. However, drillers have to find a balance between vibration reduction and drilling performance, as different rock formations and different drilling conditions often place conflicting demands on bit design. This problem becomes particularly relevant when a single bit is driven through heterogeneous, discontinuous or fractured rock formations with variable mechanical properties (Zhang et al., 2023; Kang et al., 2023).

A number of technical measures, methods, and devices have been proposed to reduce the harmful effects of vibrations and regulate the dynamic mode of the drill string (Zribi et al., 2022; Liu et al., 2023). Special devices for reducing vibrations and regulating the dynamics of the drilling tool deserve particular attention (Svitlytskyi et al., 2023; Liu et al., 2023; Velichkovich, A. & Velichkovich, S., 2001). In fact, in the practice of drilling deep wells, good results have been shown by drill string vibration absorbers and elastic spindles of downhole motors designed to absorb one or more types of vibrations (Yongwang et al., 2023; Aarsnes et al., 2019; Velichkovich & Dalyak, 2015). Typically, drill string vibration absorbers are installed between the bit and drill collars or between the bit and downhole motor, which does not exclude the possibility of installing them in other places of the drill string, for example, to perform purely technological or local protection tasks (Riane et al., 2022; Velichkovich, 2007; Velichkovich et al., 2011).

The effectiveness of such vibration protection systems is mainly determined by the strength, stiffness and damping of the elastic element. To solve the issue of vibration protection in a particular situation, it is necessary to rationally select these parameters at the design stage – to reduce the stiffness of elastic elements without compromising their strength and provide the required level of damping. When it comes to elastic elements for drilling shock absorbers, their cross-sectional dimensions are limited by the diameter of the borehole, and they are subjected to high static and dynamic loads, and sometimes temperature effects and interaction with abrasive and aggressive media are added to this. In such difficult operating conditions, plate and shell elastic elements (Shats'kyi et al., 2021; Velychkovych, 2022; Dutkiewicz et al., 2022) and magnetorheological dampers (Saleh et al., 2021; Shatskyi & Velychkovych, 2023) have proven to be efficient and effective at the same time. Similar problems associated with the occurrence of abnormal vibration loads often have to be solved at oilfields when producing oil with submersible pumps (Ma & Dong, 2023; Kopei et al., 2023). The abrasive environment with which individual shock absorber elements are in active contact leads to rapid wear of steel parts, therefore, protective functional (Dubei et al., 2022; Ropyak et al., 2023) and functional-gradient coatings are applied to their surface (Shats'kyi et al., 2019).

Drilling with PDC bits is currently the most effective option for rock destruction for the construction of oil and gas and geothermal wells (Deng et al., 2023). However, as the drilling depth increases, rock formations have higher strength and abrasiveness, worse drillingability, and more frequent interlayering and heterogeneity, which can lead to strong vibration of the PDC bit. Especially dangerous for screw motors, threaded connections and drilling tools are self-excited vibrations, which can lead to dysfunctions such as stick-slip and whirling (Nüsse et al., 2023; Tian & Detournay, 2021).

Classical drill shock absorbers were mainly designed to dampen only longitudinal vibrations (Yongwang et al., 2023; Shatskyi & Velychkovych, 2019). To protect the equipment from overloading with excessive torque and torsional vibrations, the drill shock absorber must be equipped with a unit that converts the rotational motion of its body parts into translational motion of the barrel. Due to this, sharp changes in torque will be transformed into a change in axial force acting on the shock absorber's elastic element. It is proposed to use a multiple-thread self-releasing screw pair with a trapezoidal profile of turns as a mechanism for transmitting the axial load and torque to the shock absorber. Under operating load, frictional contact interaction occurs between the screw pair elements. The result of such contact interaction will obviously have a significant impact on the peculiarity of load transfer to the elastic element, as well as on the strength of the parts of the proposed assembly.

One of the fundamental problems of a screw pair is the metrology of real precise characteristics and prediction of force interaction and the real contact area and contact stresses between the interacting surfaces (Li et al., 2022; Tutko et al., 2021). Despite the rapid development of numerical modelling methods, analytical solutions still play an important role in modelling friction pairs (Popadyuk et al., 2016; Lozynskyi et al., 2024). They can be used as a benchmark for numerical methods to achieve an "analytical understanding" of contact problems and for the proper design of virtual experiments (Grabon et al., 2018).

The article is aimed at: constructing numerical and analytical models of the mechanism for transmitting axial load and torque of a drill shock absorber; studying the dependence of the load transmitted to the elastic element of the shock absorber on changes in external torque; analysing contact stresses on interacting surfaces and assessing the strength of the parts of the proposed assembly.

2. Materials and Methods

2.1. Design features of the drill shock absorber

Now the design features of the proposed drilling shock absorber, as well as its main components, assembly units and their interaction with each other, are considered. Fig. 1 shows the general view of the shock absorber in section, additionally, two

main components of the shock absorber are highlighted: on the right – the elastic element block; on the left – the mechanism for transmitting external torque and axial load to the elastic element. The shock absorber unit consists of a set of disc springs that are arranged in series. The unit for transmitting external torque to the elastic element is a fourteen-thread, self-releasing screw pair with a trapezoidal helical profile.

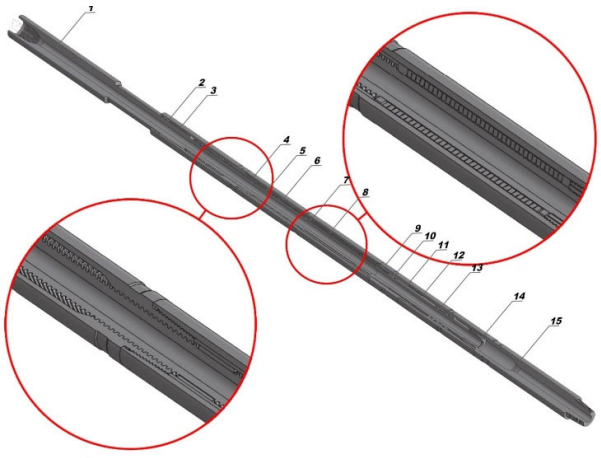

Fig. 1. Drill shock absorber for damping longitudinal and torsional vibrations

1 – shock absorber shaft with multi-thread; 2 – shaft housing with multi-thread; 3 – lower split bearing; 4 – elastic element housing; 5 – split ring; 6 – bushing; 7 – pressure ring; 8 – disc springs; 9 – lower split bearing; 10 – inner shaft; 11 – adapter connector; 12 – piston adapter; 13 – sealing piston; 14 – safety nut; 15 – upper adapter.

The shaft 1 consists of a lower part with a locking connection thread, a polished stem with a protective coating that contacts the rubber seals in the housing 2, and a working section with a screw surface. The shaft body 2 has seats for several rubber sealing elements and a split bearing 3 and has a section with a screw surface. The screw surfaces of the shaft 1 and housing 2 form a multi-thread screw pair. The split bearing 3 acts as a lower plain bearing when the shock absorber housing is rotated relative to the output shaft. The body of the elastic element 4 contains an intermediate plain bearing assembly and a package of disc springs 8. The split ring 5 and the bushing 6 act as an intermediate plain bearing, they absorb radial loads and ensure the centring of the output shaft. The pressure ring 7 is the intermediate link between the thrust shoulder of the output shaft and the spring pack. This pressure ring transfers the load from the screw pair to the spring assembly. The other end of the elastic element is fixed by a thrust ring, which is supported by an adapter connector 11. The spring element 8 ensures the necessary flexibility of the system and dissipates the energy of torsional vibrations. The split bearing of the inner shaft 9 centres and absorbs the radial loads from the inner shaft of the drill shock absorber 10. The inner shaft 10 is a continuation of the output shaft 1 and carries the sealing piston 13. An adapter 11 connects the body of the elastic element 4 and the piston adapter 12. The inner space of the piston adapter 12 contains the sealing piston 13, which can be either a bushing or a polished surface with a protective coating. The sealing piston 13 is the upper sealing unit and pressure compensator in the lubricant-filled chamber of the drilling tool. The safety nut 14 is a stroke limiter of the inner shaft 10 relative to the sealing piston 13, it prevents the piston from moving outside the working area. The upper adapter 15 is equipped with a connection thread, i.e. it is an adapter from a special thread to a lock thread. The disc springs used to form the elastic element have a high load-bearing capacity, are reliable, suitable for use at elevated temperatures and, when properly designed, provide optimum settlement and damping. To extend the warranty period, the shock absorber is sealed and filled with grease. A pressure compensation system is also used to eliminate the influence of hydrostatic pressure in the well.

When deepening a well with a combined or rotary method using PDC bits, torque fluctuations and momentary jamming of the bit with subsequent acceleration of its rotation (Stick-Slip phenomenon) are quite common. This is usually due to the fact that the geological section is represented by interlayers and inclusions of rocks with different physical and mechanical properties. Another factor is the design of PDC bits (the presence of blades that can sometimes go too deep into the rock), as well as the choice of a high axial load on the bit to ensure high mechanical drilling speed.

The Stick-Slip phenomenon can be eliminated by preventing the bit from jamming during drilling. Above, we have identified three main causes of tool jamming: high axial load; aggressive bit design; and rock characteristics. While we have no influence on the last two factors, the first one (axial load) can be influenced if we consider the proposed tool as a kind of axial load regulator. Such load control is carried out by changing the length of the drill shock absorber in case of excessive growth of the external torque. Let's imagine that while working on the bottom of a well, the bit blades have gone too deep into the rock layer, or have encountered a layer of very strong rock and the bit has jammed. The drillstring continues to rotate at a constant speed, causing the torque applied to the drilling tool to increase dramatically. The proposed shock absorber reacts instantly to these changes. The housing 2 starts to rotate relative to the output shaft 1 and, depending on the amount of increase

in external torque, this rotation can be carried out until the shaft moves to the uppermost position, thus reducing the length of the tool and the drill string as a whole. The screw pair (output shaft 1 – body 2) converts the torque increase into a force that compresses the elastic element and essentially lifts the bit by the amount of the elastic element's deflection 8. The axial load on the bit is reduced, the depth of the blades in the rock becomes smaller and the bit continues to rotate. As soon as the external torque returns to normal, all moving parts of the shock absorber return to their original position. Such a drill shock absorber can also be classified as a device for automatically adjusting the axial load and torque on the bit.

2.2. Analytical model of the axial load and torque transmission unit of a drill shock absorber

To select the right type and required characteristics of the elastic element of the drill shock absorber, it is necessary to be able to accurately determine the loads that will act on this assembly during operation. The design of the proposed drill shock absorber involves the use of a special mechanism for transmitting axial load and torque to the elastic element (Fig. 2). This special mechanism is presented in the form of a fourteen-thread self-releasing screw pair with a trapezoidal profile of turns.

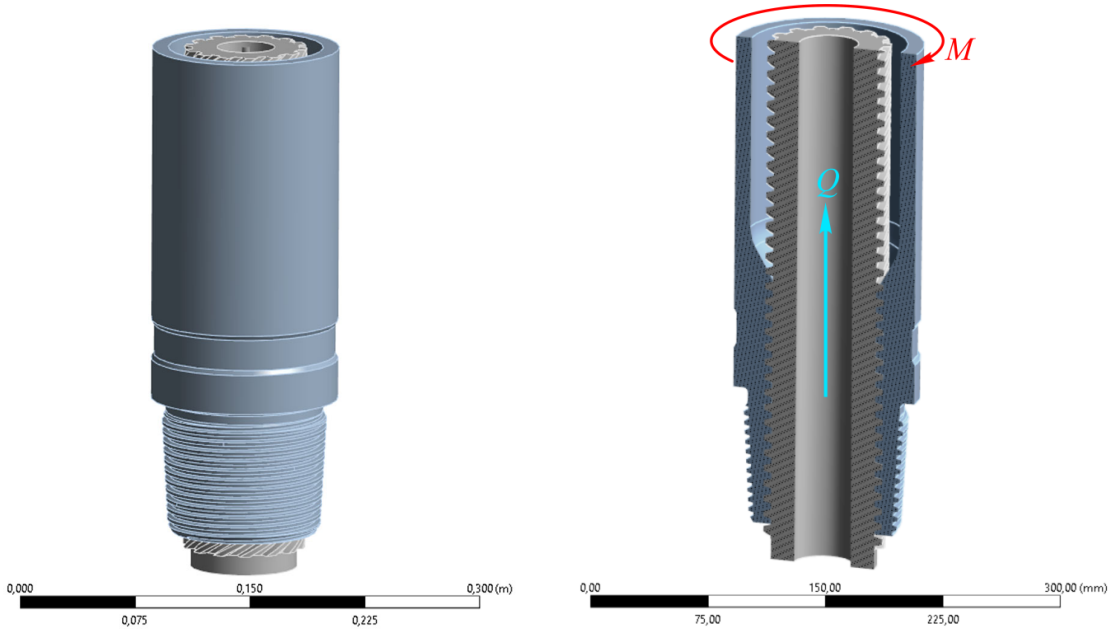

Fig. 2. General view (a) and longitudinal section (b) of the axial load and torque transmission unit in the drill shock absorber

Now consider a situation where the bit at the bottom of a well has slowed down (or stopped) due to excessive rock resistance. Suppose that an additional external torque M is applied to the shock absorber body parts. It tries to rotate the shock absorber body parts relative to the shaft and causes the contact interaction of the screw pair elements. The screw pair transforms the applied torque into an axial force Q, which compresses the elastic element of the shock absorber, causing its settlement Δ. Let us consider the force interaction between the elements of a screw pair based on the model of Fig. 2. Let us imagine that one thread of the screw thread is untwisted by one revolution (Fig. 2, a). In this case, one edge of the thread forms the hypotenuse of a right triangle, the base of which is equal to the circumference of the circle of average radius R of the screw pair, and the height of such a triangle is equal to the thread pitch h multiplied by the number of turns n. Angle α is the angle of rise of the cut. The conditions of frictional interaction on the contact surfaces are taken in the form of Coulomb's law. The external torque M causes a circular force in the screw pair $P = M / R$. On the contacting surfaces, the contact pressure force N is directed along the normal to the cut surfaces, and the friction force F acts in a plane tangent to the cut surface (Fig. 2, b and Fig. 2, c).

Now we will determine the relationship between the external torque M and the force Q compressing the elastic element of the shock absorber. Then, we write the equilibrium equation for the shaft model (Fig. 2, b), taking into account that the profile of the screw pair's turns is trapezoidal (Fig. 2, d):

$$\sum Y_i = -Q + N\cos\beta\cos\alpha - F\sin\alpha = 0. \quad (1)$$

Equilibrium equation for the housing model (Fig. 2, c)

$$\sum X_i = -P + N\cos\beta\sin\alpha + F\cos\alpha = 0. \quad (2)$$

In the process of jointly solving the system of Eq. (1) and Eq. (2), we multiply Eq. (2) by R, moving from forces to moments, and also take into account that the friction force is determined by the formula $F = fN$, where f – is the friction coefficient on the contact surfaces of the screw connection. As a result, we obtain:

– force Q, that loads the elastic element

$$Q = \frac{M}{R} \cdot \frac{\cos\alpha\cos\beta - f\sin\alpha}{\sin\alpha\cos\beta + f\cos\alpha}; \tag{3}$$

– contact pressure resultant

$$N = \frac{M}{R} \cdot \frac{1}{\sin\alpha\cos\beta + f\cos\alpha}; \tag{4}$$

– friction forces resultant

$$F = f\frac{M}{R} \cdot \frac{1}{\sin\alpha\cos\beta + f\cos\alpha}. \tag{5}$$

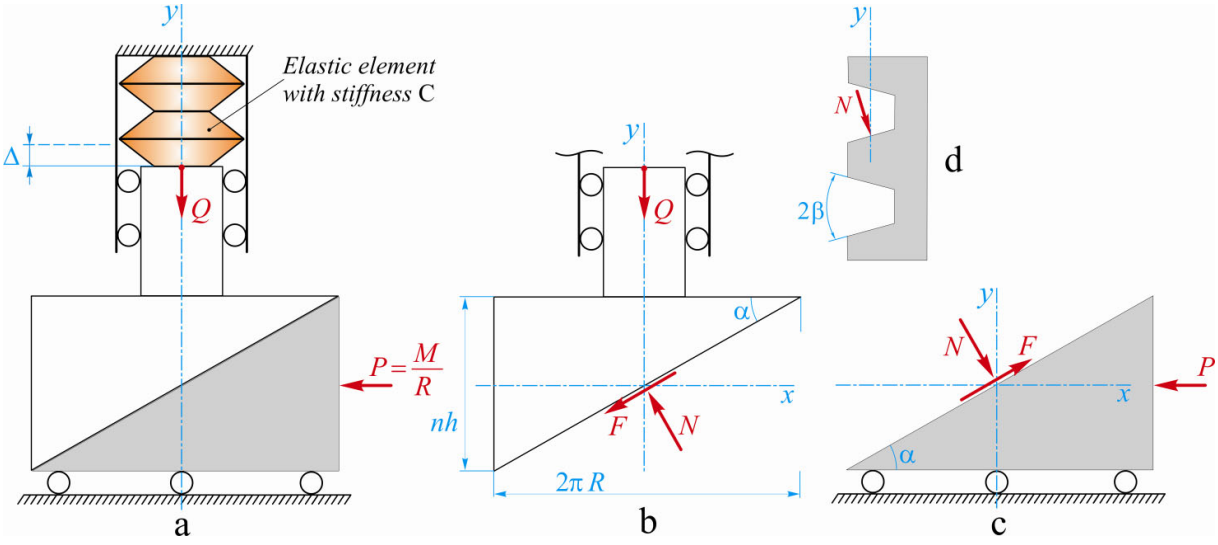

Fig. 3. Model of force interaction in the system screw pair – elastic shock absorber element: a – design diagram of the analytical model; b – shaft loading diagram; c – housing loading diagram; d – profile of the screw pair's threads.

Excluding from formula (3) the trigonometric functions of the angle of thread rise, after the transformations, we obtain the final form of the dependence of the axial load Q, which is transmitted to the elastic element of the shock absorber, on the change in the external torque M:

$$Q = \frac{M}{R} \cdot \frac{1 - f\dfrac{nh}{2\pi R}\sec\beta}{\dfrac{nh}{2\pi R} + f\sec\beta}. \tag{6}$$

If the drill shock absorber is loaded with external axial force P_0 only, a torque T will occur in the screw pair, which can be determined by the formula

$$T = P_0 R \cdot \frac{f\sec\beta - \dfrac{nh}{2\pi R}}{1 + f\dfrac{nh}{2\pi R}\sec\beta}. \tag{7}$$

This moment T will contribute to the formation of the load value of the elastic element. To calculate this contribution, it is enough to substitute the value of T calculated by formula (7) in formula (6) instead of the value of M. After performing the above steps, we obtain an expression for determining the force Q_0, transmitted to the elastic element when the shock absorber is loaded only by an external axial force P_0:

$$Q_0 = -P_0 \frac{f \sec\beta - tg\alpha}{1 + f \sec\beta \; tg\alpha} \cdot \frac{1 - f \sec\beta \; tg\alpha}{f \sec\beta + tg\alpha}. \tag{8}$$

In the case when the shock absorber is simultaneously subjected to an external torque *M* and an external axial load P_0, it is necessary to first use formula (7), and then in formula (6), instead of *M*, substitute the sum of $M + T$.

During the operation of the shock absorber, normal σ and tangential τ_c contact stresses will act on the surface of the screw threads

$$\sigma = \frac{M}{\pi R^2 h} \cdot \frac{\cos\beta \cos\alpha}{\sin\alpha \cos\beta + f \cos\alpha}, \tag{9}$$

$$\tau_c = f \frac{M}{\pi R^2 h} \cdot \frac{\cos\beta \cos\alpha}{\sin\alpha \cos\beta + f \cos\alpha}, \tag{10}$$

and shear stresses τ_s will act in the cross-section of the turns

$$\tau_s = \frac{M}{\pi R^2 h} \cdot \frac{\cos\alpha}{\sin\alpha \cos\beta + f \cos\alpha}, \tag{11}$$

here, according to the standard for a trapezoidal cut profile, it is assumed that the height of the contact surface of the turn and the average width of the turn are equal 0.5*h*. Since a complex stress state occurs in the dangerous points of the screw pair material, we will use the Huber-von Mises energy criterion to assess the strength. To ensure strength, it is necessary that the highest equivalent stresses σ_{eq}, that occur in the material during operation do not exceed the permissible stresses $[\sigma]$:

$$\sigma_{eq} = \frac{1}{\sqrt{2}} \sqrt{\sigma^2 + 6(\tau_c^2 + \tau_s^2)} \le [\sigma]. \tag{12}$$

To check the strength of a screw pair, it is necessary to first use formulas (9)-(11), and then check the fulfilment of the inequality (12).

2.3. Numerical model of the axial load and torque transmission unit of a drill shock absorber

To verify the adequacy of the proposed analytical model and verify certain analytical results, we decided to use a numerical model of the axial load and torque transmission unit of the drill shock absorber. The deformable bodies in contact were represented as separate arrays of finite elements with a certain number of nodes in the contact area (Fig. 4).

Ansys Workbench 2022 R2 modules were used to build the model and obtain results. The calculation mesh for the screw connection parts was generated using the Tetrahedrons method. The advantage of the tetrahedral mesh is that it allows for a good approximation of the surface contour, and it is also recommended for modelling contact problems. In the process of forming the finite element model, a mesh independence study was performed using the methodology recommended by Ansys (Stolarski et al., 2018). As a result, three-dimensional meshes with elements in the form of tetrahedra with an average edge length of 3 mm were obtained for both parts of the screw connection (in the areas of the cut, the mesh was refined). For the generation process, we used the "Patch Independent" method, which is convenient because it overlays the mesh on the design area and then cuts off all fragments that go beyond the geometric area.

The mechanical and geometrical parameters of the screw connection are as follows. The material of the shaft and the shock absorber housing is structural alloy steel with yield strength $480 MPa$, Young's modulus – $2.1 \cdot 10^{11} Pa$, shear modulus – $8 \cdot 10^{10} Pa$ and Poisson's ratio – 0.31. The outer diameter of the screw connection is 80 mm, the average diameter is 75 mm, the number of threads is 14, and the pitch is 10 mm.

The following software parameters were used to describe the contact interaction of screw pair parts: contact type – “Frictional” with a friction coefficient of 0.05 (this coefficient was changed in the course of the study); contact formulation – “Augmented Lagrange method”; 0.0015 penetration tolerance; normal stiffness factor on the contact surfaces – “Program controlled”. It should be noted here that the Augmented Lagrange method was chosen because this method allows for minimal penetration of the contact surfaces, but at the same time ensures the reliability of the results and acceptable computational time.

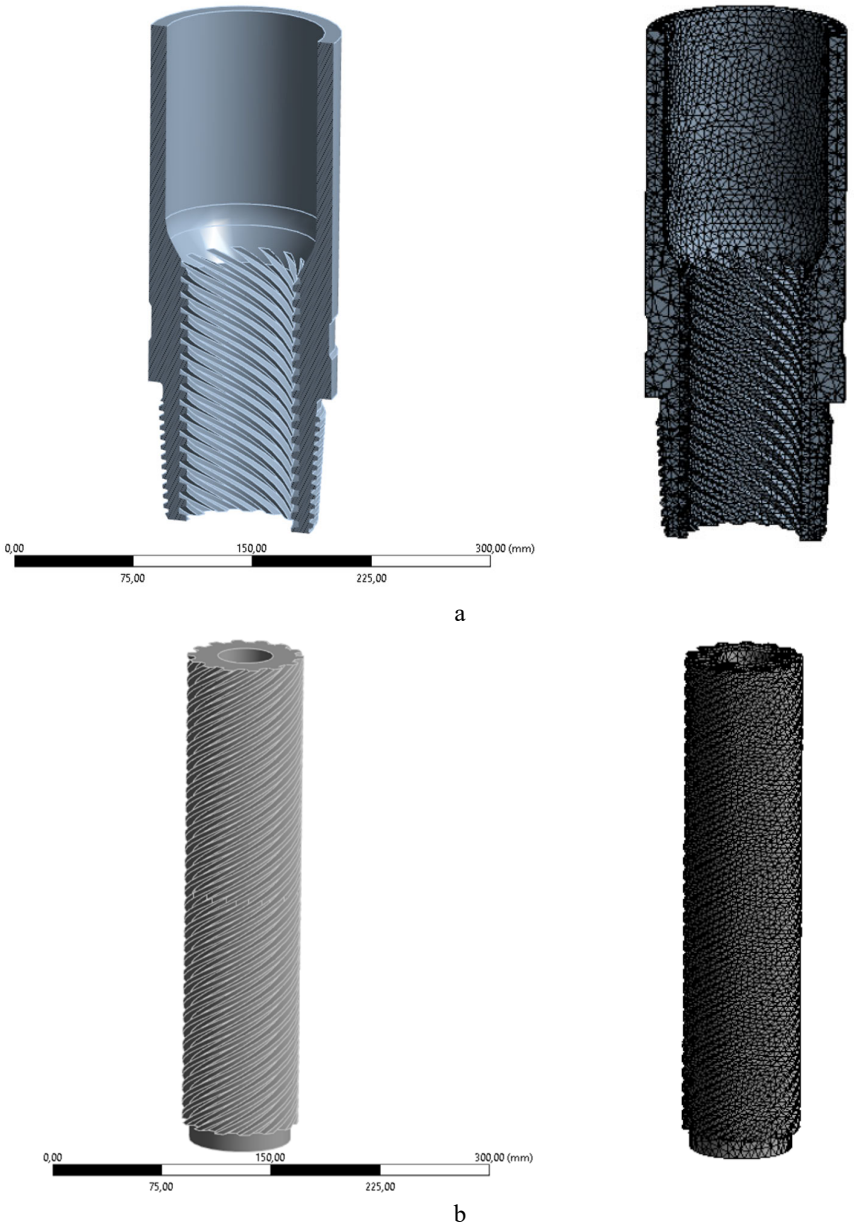

Fig. 4. Finite element models of a part of the shock absorber body (a) and a part of the shock absorber shaft (b)

In total, the created model of the screw pair contains 521801 finite elements. To obtain numerical solutions, a step-by-step loading process was used, with the boundary conditions refined at each loading step using an iterative method. The study mainly evaluated the ability of the screw pair to transform external torque into axial force, while controlling the values of contact pressures, axial displacements, and equivalent stresses. The load increases were chosen to be small in order to maintain a close to linear relationship between displacements and deformations within each load step.

3. Results and Analysis

The main feature of the proposed mechanism for transmitting axial load and torque in the shock absorber is that, under certain circumstances, it is capable of converting the rotational movement of the shock absorber body parts into translational movement of the barrel (or vice versa). In this case, the excessive increase in external torque is transformed into an axial force that is transmitted to the elastic element. Excessive torque increase can be caused by slowing down or jamming of the bit due to strong blade penetration into the rock, rock layering or fracturing, abrupt change in the mechanical properties of the rock, etc. It should be noted that the barrel, compressing the elastic element, raises the bit above the bottomhole surface by the amount of the elastic element's upsetting and thus allows the bit to continue rotating in the nominal mode.

The analytical dependence between the change in the external torque M and the value of the axial load Q compressing the elastic element of the drill shock absorber is analysed. In Fig. 5, the graphical results of the force interaction in a screw

pair are presented in a dimensionless form, since in this case, a whole group of possible dimensional problems corresponds to one solved dimensionless variant. The graphs in Fig. 5, a demonstrate the change in the load on the elastic element depending on the friction coefficient on the contact surfaces of the screw pair. With an increase in the friction coefficient, the load on the elastic element decreases, and this dependence is non-linear. All other things being equal, screws with fewer threads are more sensitive to changes in the coefficient of friction. The graphical dependencies in Fig. 5, b illustrate how the load on the shock absorber's elastic element will change with changes in the geometric parameters of the screw pair. With an increase in the ratio h / R – the force that will compress the elastic element will decrease, and this dependence is non-linear. All other things being equal, screws with a higher coefficient of friction on the contact surfaces are more sensitive to changes in geometric parameters.

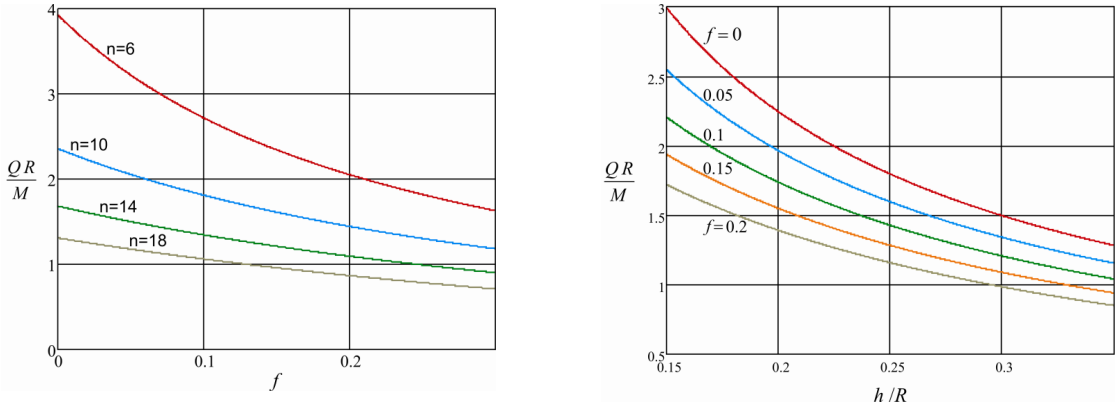

a b

Fig. 5. Changes in the load transferred to the shock absorber's elastic element: a – depending on the friction coefficient on the contact surfaces of the screw pair (we accept $h / R = 0.26$); b – depending on the geometrical parameters of the screw pair (we accept $n = 14$)

The numerical results shown in Fig. 6 are obtained for a real drill shock absorber with an outer diameter of 121 mm, which is planned to be used for drilling for production strings. The parameters of the screw connection are as follows: outer diameter of the screw connection thread is 80 mm, average diameter is 75 mm, number of threads is 14, pitch is 10 mm. As the external torque M increases, the axial force Q acting on the elastic element increases linearly. With a decrease in the coefficient of friction on the contact surfaces, the resistance forces in the screw connection decrease and, as a result, the load on the elastic element increases.

The next numerical testing of the model was focused on determining the settlement of the elastic element caused by an increase in external torque. Both the finite element and analytical models were used for calculations, and the results were compared. In both cases, the shock absorber barrel loaded a linear elastic element with a stiffness of $C = 2000\ kN / m$. In the numerical model (Fig. 7, a), a virtual tensile spring was used, the upper end of which was connected to the upper end of the barrel (shown in green), and the lower end of the spring was fixed in space (the reaction in the fixation and the local coordinate system are shown). As for the boundary conditions, the lower end of the barrel is not allowed to rotate (this corresponds to the case of bit jamming), while the body is only allowed to rotate about the longitudinal axis.

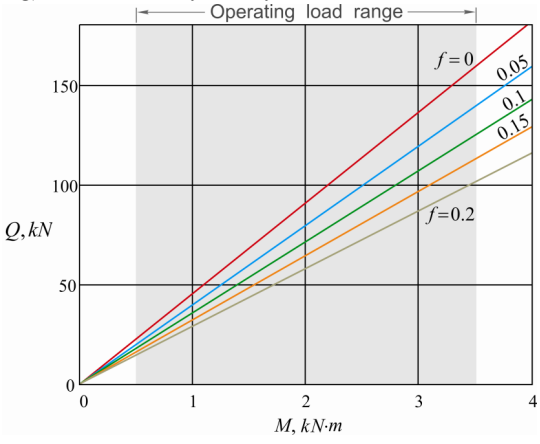

Fig. 6. Dependence of the force compressing the shock absorber elastic element on the external torque

An external torque was applied to the body and the elongation of the virtual spring Δ was measured. In the analytical model (Fig. 3, a), we took into account that $\Delta = Q/C$. The analytical model (Fig. 7, b) gives slightly overestimated results for the settlements, and the percentage of discrepancy between the results increases with increasing external load. For example, when an external torque of 500 kNm was applied, the discrepancy between the analytical and numerical results was 8%, and at 3500 kNm the discrepancy increased to 12%. It should also be noted that with the installation of a stiffer elastic element and a reduction in the displacements in the screw pair, the discrepancy between the numerical and analytical results decreases.

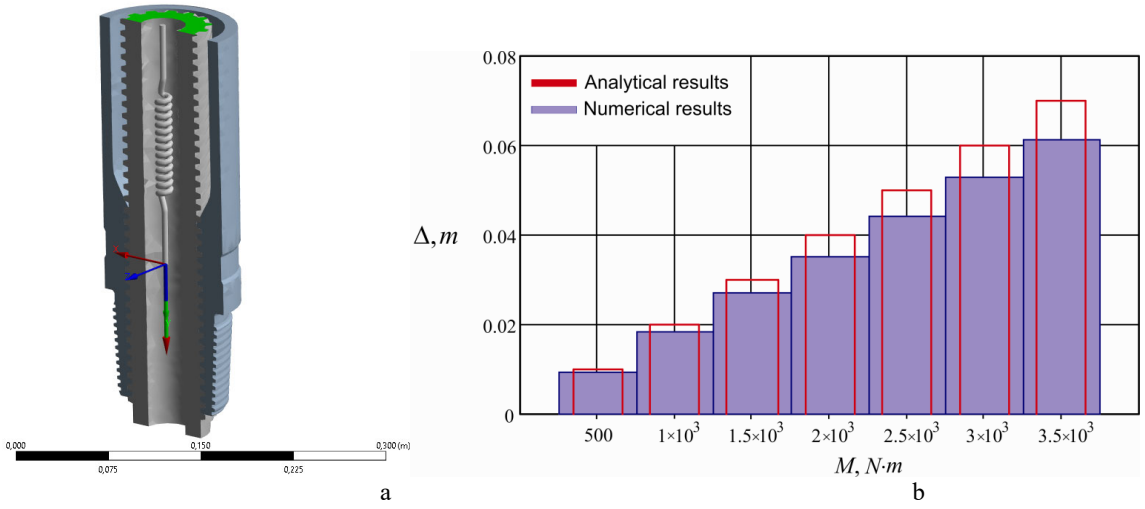

Fig. 7. Determination of the settlement of an elastic element caused by an external torque (friction coefficient on contact surfaces is 0.05): a – virtual model of a screw pair; b – comparison of numerical and analytical results

If the drill shock absorber is loaded with an external axial force P_0, only a certain part of it Q_0 will load the elastic element of the shock absorber, the rest will be used to overcome the drag forces in the screw pair. The relationship between P_0 and Q_0 is illustrated graphically in Fig. 8. Obviously, with the growth of the friction coefficient, the resistance forces in the screw pair increase, and the load transmitted to the elastic element decreases accordingly.

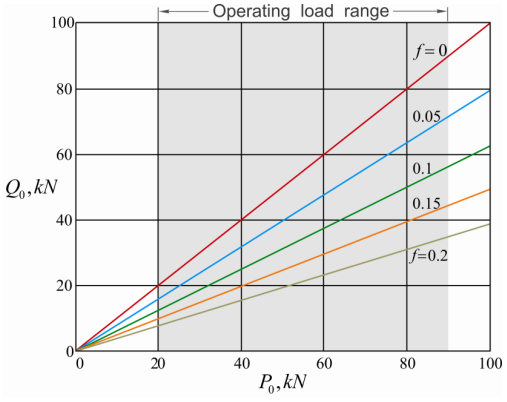

Fig. 8. Relationship between the external axial force P_0 and the force Q_0, transmitted to the shock absorber elastic element

To assess the strength of a screw pair, the stressed state of its parts in response to an external load was considered. It was found that the highest equivalent stresses occur on the surfaces of the threads. The analytical results presented in Fig. 9, were obtained on the basis of formulas (9)–(12). To verify the analytical results obtained, the following virtual experiment was conducted (Fig. 10). An external torque $M = 1000\ kN$ was applied to the housing, which is only allowed to rotate around the longitudinal axis. The lower end of the shaft was prevented from rotating, and a smooth barrier was placed in front of the upper end of the shaft. The housing, rotating around its longitudinal axis, forced the shaft to move progressively in the axial direction and press with a force Q against the smooth barrier. Fig. 10 shows the contact pressure chromograms on the interacting surfaces and the equivalent stress chromograms in the screw connection parts.

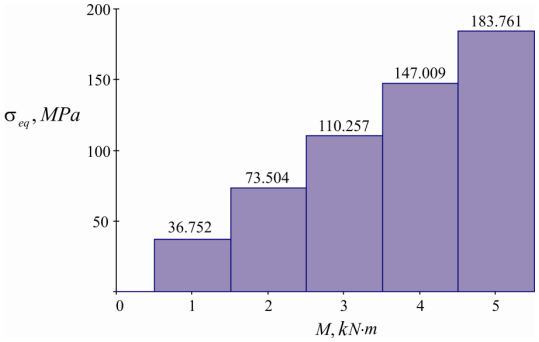

Fig. 9. The largest equivalent stresses in a screw pair (analytical result)

The general picture of the contact pressure distribution on the surfaces of the screw pair in contact interaction is shown in Fig. 10, a (here the internal part – the shaft is shown transparent). The distribution of contact pressures between the turns of the screw pair is fairly uniform, which means that the external load will be distributed between all turns of the contact pair. The contact pressure is unevenly distributed along the length of the turn, with disturbances at the beginning and end of each turn, which is likely to lead to faster wear of these particular parts of the screw connection turns.

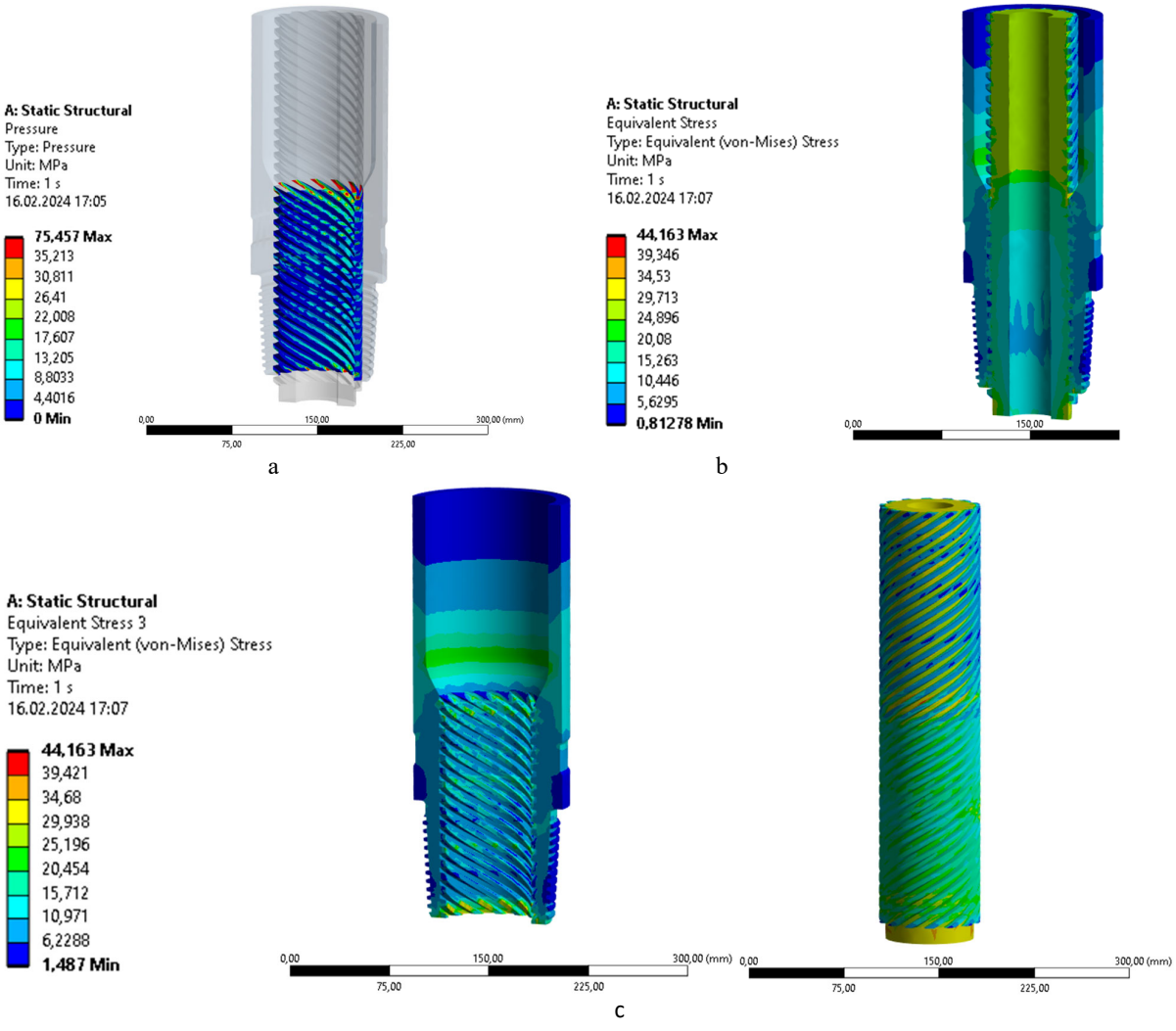

Fig. 10. Results of the virtual experiment: a – contact pressure on the interacting surfaces; b – equivalent stresses in the screw connection; c – equivalent stresses in the screw connection parts

Figs. 10, b and 10, c show a general picture of the distribution of equivalent stresses in the material of the connection parts. The equivalent stresses were calculated using the Huber-von Mises energy theory of strength. The resulting chromograms show that all turns of the screw pair are involved. If we exclude from the calculation several singularity points that occur on the equivalent stress chromograms, the value of the maximum equivalent stresses should be taken as the lower limit of the stress range, which is marked in red on the numerical scale. This value is 39.4 MPa and is in good agreement with the analytical result shown in Fig. 9 (see value of σ_{eq} when $M = 1000\,N \cdot m$).

If in the virtual experiment, the results of which are shown in Fig. 10, we increase the external load by a factor of 5, we will get the results shown in Fig. 11.

Under high torque loading of a screw pair, the maximum equivalent stresses occur in the lower parts of the turns, while all the turns of the connection are in a similar stress state. This means that the external load is distributed approximately evenly across all the connection turns, but the lower parts of the turns will experience faster wear.

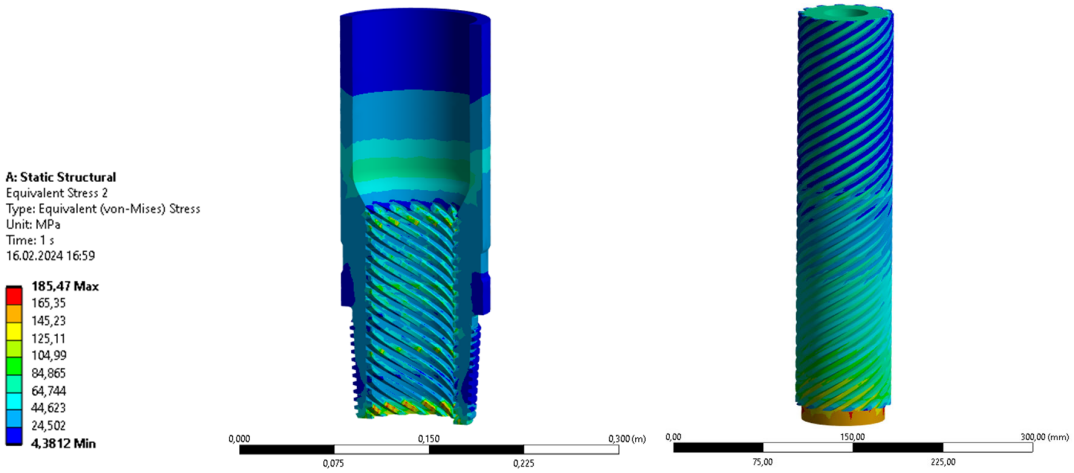

Fig. 11. The case of a high-torque operating load of a screw pair (external torque applied $M = 5000\,N \cdot m$)

Comparing the maximum value of the equivalent stresses – $185.47\,MPa$ (Fig. 11) with the value obtained analytically – (see Fig. 9 for the value of σ_{eq} when $M = 5000\,N \cdot m$) we see a good convergence of the results obtained in different ways. Recall that the material of the shock absorber shaft and housing is structural alloy steel with yield strength $480\,MPa$. This value is higher than the maximum equivalent stresses that occur under high torque loading of the screw pair, and therefore the ultimate state of the structure is not reached. By dividing the yield strength of the material by the maximum equivalent stress, the actual safety factor with which the screw pair is operated is obtained.

4. Conclusions

The paper proposes an improved shock absorber design for use in the drilling of deep oil and gas and geothermal wells when rock destruction occurs using PDC bits. The drill shock absorber is equipped with a unit that converts the rotational motion of its body parts into the translational motion of the barrel. As a result, sudden changes in external torque are transformed into a change in the axial force that loads the shock absorber's elastic element. Due to its new properties, the shock absorber is able to prevent self-excited vibrations, which can lead to dysfunctions such as stick-slip and whirling of the drilling tool.

The numerical and analytical models of the mechanism of transferring external axial load and torque to the elastic element of a drill shock absorber are constructed. An analytical dependence was obtained to determine the value of the load transmitted to the elastic element of the drill shock absorber when the external torque changes. This result will allow for an efficient selection of the characteristics of the elastic element for a drill shock absorber. An analytical assessment of the strength of the shock absorber screw pair was carried out using the Huber-von Mises energy criterion.

Using a numerical model of a screw pair, the distribution of contact pressures on the interacting surfaces and equivalent stresses in the details of the proposed assembly is analysed. It has been determined that the external load is evenly distributed between all turns of the screw pair, and under high-torque operating load the limit state of the assembly parts is not reached. A numerical estimation of the value of the shock absorber elastic element's settlement, which occurs under the action of an

external torque, has been carried out. The identification of a number of results obtained by the finite element method with the results of analytical solutions allows us to recommend the proposed analytical model for practical applications.

References

Aarsnes, U. J. F., & van de Wouw, N. (2019). Effect of shock subs on self-excited vibrations in drilling systems. *Journal of Petroleum Science and Engineering, 181*, 106217. https://doi.org/10.1016/j.petrol.2019.106217

Bembenek, M., Grydzhuk, Y., Gajdzik, B., Ropyak, L., Pashechko, M., Slabyi, O., Al-Tanakchi, A., & Pryhorovska, T. (2024). An Analytical–Numerical Model for Determining "Drill String–Wellbore" Frictional Interaction Forces. *Energies, 17*(2), 301. https://doi.org/10.3390/en17020301

Deng, P., Tan, X., Bai & Li, H. (2023). Influence of Blades' Shape and Cutters' Arrangement of PDC Drill Bit on Nonlinear Vibration of Deep Drilling System. *Journal of Sound and Vibration*, 118165. https://doi.org/10.1016/j.jsv.2023.118165

Dubei, O. Y., Tutko, T. F., Ropyak, L. Y., & Shovkoplias, M. V. (2022). Development of Analytical Model of Threaded Connection of Tubular Parts of Chrome-Plated Metal Structures. *Metallofizika i noveishie tekhnologii, 44*(2), 251–272. https://doi.org/10.15407/mfint.44.02.0251

Dutkiewicz, M., Velychkovych, A., Shatskyi, I., & Shopa, V. (2022). Efficient Model of the Interaction of Elastomeric Filler with an Open Shell and a Chrome-Plated Shaft in a Dry Friction Damper. *Materials, 15*(13), 4671. https://doi.org/10.3390/ma15134671

Grabon, W. A., Osetek, M., & Mathia, T. G. (2018). Friction of threaded fasteners. *Tribology International, 118*, 408–420. https://doi.org/10.1016/j.triboint.2017.10.014

Grydzhuk, J., Chudyk, I., Velychkovych, A., & Andrusyak, A. (2019). Analytical estimation of inertial properties of the curved rotating section in a drill string. *Eastern-European Journal of Enterprise Technologies, 1*(7–97), 6–14. https://doi.org/10.15587/1729-4061.2019.154827

Haige, W., Hongchun, H., Wenxin, B., Guodong, J., Bo, Z., & Lubin, Z. (2022). Deep and ultra-deep oil and gas well drilling technologies: Progress and prospect. *Natural Gas Industry B, 9*(2), 141–157. https://doi.org/10.1016/j.ngib.2021.08.019

Kang, M., Hua, D., & Guo, X. (2023). Review on the Influence of Complex Stratum on the Drilling Trajectory of the Drilling Robot. *Applied Sciences, 13*(4), 2532. https://doi.org/10.3390/app13042532

Kopei, B., Kopei, I., Kopei, V., Onysko, O., & Mykhailiuk, V. (2023). Comparison of the Main Parameters of the Steel and Carbon-Fiber-Reinforced Plastic Band Traction Units for Long-Stroke Oil Well Pumps. In: Karabegovic, I., Kovačević, A., Mandzuka, S. (eds) New Technologies, Development and Application VI. NT 2023. *Lecture Notes in Networks and Systems, 687*. Springer, Cham. https://doi.org/10.1007/978-3-031-31066-9_10

Li, B., Li, P., Zhou, R., Feng, X.-Q., & Zhou, K. (2022). Contact mechanics in tribological and contact damage-related problems: A review. *Tribology International, 171*, 107534. https://doi.org/10.1016/j.triboint.2022.107534

Li, G., Song, X., Tian, S., & Zhu, Z. (2022). Intelligent Drilling and Completion: A Review. *Engineering.* https://doi.org/10.1016/j.eng.2022.07.014

Liu, Q., Zhou, B., Chen, F., Li, N., Xie, J., Zhao, M., Di, Q., Feng, C., Song, S., & Yin, C. (2023). Optimal design and nonlinear dynamic characteristics of titanium /steel drill pipe composite drill string for ultra-deep drilling. *Scientific Reports, 13*(1). https://doi.org/10.1038/s41598-023-47156-y

Liu, Y., Niu, Y., Guan, Z., & Lyu, S. (2022). The Review and Development of Devices with an Increasing Rate of Penetration (ROP) in Deep Formation Drilling Based on Drill String Vibration. *Energies, 15*(19), 7377. https://doi.org/10.3390/en15197377

Lozynskyi, V., Shihab, T., Drach, I., & Ropyak, L. (2024). The Inertial Disturbances of Fluid Movement in the Chamber of a Liquid Autobalancer. *Machines, 12*(1), 39. https://doi.org/10.3390/machines12010039

Ma, B., & Dong, S. (2023). Coupling Simulation of Longitudinal Vibration of Rod String and Multi-Phase Pipe Flow in Wellbore and Research on Downhole Energy Efficiency. *Energies, 16*(13), 4988. https://doi.org/10.3390/en16134988

Mao, L., He, J., Zhu, J., Jia, H., & Gan, L. (2024). Dynamic characteristic response of PDC bit vibration coupled with drill string dynamics. *Geoenergy Science and Engineering, 233*, 212524. https://doi.org/10.1016/j.geoen.2023.212524

Maury, J., Hamm, V., Loschetter, A., & Le Guenan, T. (2022). Development of a risk assessment tool for deep geothermal projects: example of application in the Paris Basin and Upper Rhine graben. *Geothermal Energy, 10*(1). https://doi.org/10.1186/s40517-022-00238-y

Nüsse, P. M., Ambrus, A., Aarsnes, U. J. F., & Aamo, O. M. (2023). Evaluation of distributed damping subs with active control for stick-slip reduction in drilling. *Geoenergy Science and Engineering*, 212255. https://doi.org/10.1016/j.geoen.2023.212255

Popadyuk, I. Yo., Shats'kyi I. P., Shopa V. M., & Velychkovych A. S. (2016). Frictional interaction of a cylindrical shell with deformable filler under nonmonotonic loading. *Journal of Mathematical Sciences, 215*(2), 243–253. https://doi.org/10.1007/s10958-016-2834-x

Riane, R., Doghmane, M. Z., Kidouche, M., & Djezzar, S. (2022). Observer-Based H∞ Controller Design for High Frequency Stick-Slip Vibrations Mitigation in Drill-String of Rotary Drilling Systems. *Vibration, 5*(2), 264–289. https://doi.org/10.3390/vibration5020016

Ropyak, L., Shihab, T., Velychkovych, A., Bilinskyi, V., Malinin, V., & Romaniv, M. (2023). Optimization of Plasma Electrolytic Oxidation Technological Parameters of Deformed Aluminum Alloy D16T in Flowing Electrolyte. *Ceramics, 6*(1), 146–167. https://doi.org/10.3390/ceramics6010010

Saadat, S., Prakasan, H., Poothia, T., Pandey, G. (2023). A comprehensive study on vibration control and evaluation of drill string during drilling operation. *AIP Conf. Proc., 2855*(1), 040009. https://doi.org/10.1063/5.0168428

Saleh, M. K. A., Nejatpour, M., Yagci Acar, H., & Lazoglu, I. (2021). A new magnetorheological damper for chatter stability of boring tools. *Journal of Materials Processing Technology, 289,* 116931. https://doi.org/10.1016/j.jmatprotec.2020.116931

Shats'kyi, I. P., & Struk, A. B. (2009). Stressed state of pipeline in zones of soil local fracture. *Strength of Materials, 41*(5), 548–553. https://doi.org/10.1007/s11223-009-9165-9

Shats'kyi, I. P., Shopa, V. M., & Velychkovych, A. S. (2021). Development of full-strength elastic element section with open shell. *Strength of Materials, 53*, 277–282. https://doi.org/10.1007/s11223-021-00286-y

Shats'kyi, I. P., Makoviichuk, M. V., & Shcherbii, A. B. (2019). Influence of a Flexible Coating on the Strength of a Shallow Cylindrical Shell with Longitudinal Crack. *Journal of Mathematical Sciences, 238*(2), 165–173. https://doi.org/10.1007/s10958-019-04226-9

Shatskyi, I., & Velychkovych, A. (2019). Increase of compliance of shock absorbers with cut shells. *IOP Conf. Ser. Mater. Sci. Eng., 564,* 012072. https://doi.org/10.1088/1757-899X/564/1/012072

Shatskyi, I., & Velychkovych, A. (2023). Analytical Model of Structural Damping in Friction Module of Shell Shock Absorber Connected to Spring. *Shock and Vibration,* 2023, 1–17. https://doi.org/10.1155/2023/4140583

Stolarski, T., Nakasone, Y., Yoshimoto, S. (2018). Application of ANSYS to contact between machine elements. *Engineering Analysis with ANSYS Software,* 2018, 375–509. https://doi.org/10.1016/B978-0-08-102164-4.00007-8

Svitlytskyi, V., Iagodovskyi, S., & Bilenko, N. (2023). Effect of vibration dampers on the dynamic state of a drill string. *Technology Audit and Production Reserves, 5*(1(73), 32–36. https://doi.org/10.15587/2706-5448.2023.290145

Tian, K., & Detournay, E. (2021). Influence of PDC bit cutter layout on stick–slip vibrations of deep drilling systems. *Journal of Petroleum Science and Engineering, 206,* 109005. https://doi.org/10.1016/j.petrol.2021.109005

Tutko, T., Dubei, O., Ropyak, L., Vytvytskyi, V. (2021). Determination of Radial Displacement Coefficient for Designing of Thread Joint of Thin-Walled Shells. Advances in Design, Simulation and Manufacturing IV. DSMIE 2021. *Lecture Notes in Mechanical Engineering. Springer, Cham,* pp. 153–162. https://doi.org/10.1007/978-3-030-77719-7_16

Velichkovich, A. S. & Dalyak, T. M. (2015). Assessment of stressed state and performance characteristics of jacketed spring with a cut for drill shock absorber. *Chemical and Petroleum Engineering, 51*(3), 188–193. https://doi.org/10.1007/s10556-015-0022-3

Velichkovich, A. S. (2007). Design features of shell springs for drilling dampers. *Chemical and Petroleum Engineering, 43*(7–8), 458–461. https://doi.org/10.1007/s10556-007-0081-1

Velichkovich, A. S., & Velichkovich, S. V. (2001). Vibration-impact damper for controlling the dynamic drillstring conditions. *Chemical and Petroleum Engineering, 37*(3–4), 213–215. https://doi.org/10.1023/A:1017650519261

Velichkovich, A. S., Popadyuk, I. I., & Shopa, V. M. (2011). Experimental study of shell flexible component for drilling vibration damping devices. *Chemical and Petroleum Engineering, 46,* 518–524. https://doi.org/10.1007/s10556-011-9370-9

Velichkovich, A., Dalyak, T., & Petryk, I. (2018). Slotted shell resilient elements for drilling shock absorbers. *Oil & Gas Science and Technology – Revue d'IFP Energies nouvelle*s, 73, 34. https://doi.org/10.2516/ogst/2018043

Velychkovych, A. (2022). Numerical model of interation of package of open shells with a weakly compressible filler in a friction shock absorber.*Engineering Solid Mechanics, 10*(3), 287-298. https://doi.org/10.5267/j.esm.2022.3.002

Vytvytskyi, I. I., Seniushkovych, M. V., & Shatskyi, I. P. (2017). Calculation of distance between elastic-rigid centralizers of casing. *Naukovyi Visnyk Natsionalnoho Hirnychoho Universytetu, 5*, 28–35.

Wang, C., Chen, W., Wu, Z., Li, J., & Liu, G. (2023). Stick–Slip Characteristics of Drill Strings and the Related Drilling Parameters Optimization. *Processes, 11*(9), 2783. https://doi.org/10.3390/pr11092783

Yavari, H., Fazaelizadeh, M., Aadnoy, B. S., Khosravanian, R., Qajar, J., Sedaghatzadeh, M., & Riazi, M. (2023). An approach for optimization of controllable drilling parameters for motorized bottom hole assembly in a specific formation. *Results in Engineering, 20*, 101548. https://doi.org/10.1016/j.rineng.2023.101548

Yongwang, L., Hongning, Z., Yixiang, N., Guojun, L., Wentao, L., & Yiwu, L. (2023). Experiment on the influence of downhole drill string absorption & hydraulic supercharging device on bottom hole WOB fluctuation. *Energy Reports, 9,* 2372–2378. https://doi.org/10.1016/j.egyr.2023.01.047

Yongwang, L., Hongning, Z., Yixiang, N., Guojun, L., Wentao, L., & Yiwu, L. (2023). Experiment on the influence of downhole drill string absorption & hydraulic supercharging device on bottom hole WOB fluctuation. *Energy Reports, 9*, 2372–2378. https://doi.org/10.1016/j.egyr.2023.01.047

Zhang, D., Yang, Y., Ren, H., Huang, K., & Niu, S. (2023). Experimental research on efficiency and vibration of polycrystalline diamond compact bit in heterogeneous rock. *Journal of Petroleum Science and Engineering, 220*, 111175. https://doi.org/10.1016/j.petrol.2022.111175

Zribi, F., Sidhom, L., Gharib, M., & Refaat, S. S. (2022). New algorithm based active method to eliminate stick-slip vibrations in drill string systems. *Systems Science & Control Engineering, 10*(1), 468–487. https://doi.org/10.1080/21642583.2022.2047123